Biochemistry

pubs.acs.org/biochemistry

Communication

Photocycle of Cyanobacteriochrome TePixJ

Samantha J. O. Hardman, Derren J. Heyes, Igor V. Sazanovich, and Nigel S. Scrutton*

Cite This: *Biochemistry* 2020, 59, 2909−2915

Read Online

ACCESS | Metrics & More | Article Recommendations | Supporting Information

ABSTRACT: Due to the recent advances in X-ray free electron laser techniques, bilin-containing cyanobacteriochrome photoreceptors have become prime targets for the ever-expanding field of time-resolved structural biology. However, to facilitate these challenging studies, it is essential that the time scales of any structural changes during the photocycles of cyanobacteriochromes be established. Here, we have used visible and infrared transient absorption spectroscopy to probe the photocycle of a model cyanobacteriochrome system, TePixJ. The kinetics span multiple orders of magnitude from picoseconds to seconds. Localized changes in the bilin binding pocket occur in picoseconds to nanoseconds, followed by more large-scale changes in protein structure, including formation and breakage of a second thioether linkage, in microseconds to milliseconds. The characterization of the entire photocycle will provide a vital frame of reference for future time-resolved structural studies of this model photoreceptor.

Time-resolved structural studies of biological systems are becoming ever more common and accessible.[1] Advances in synchrotrons and X-ray free electron lasers (XFELs) have increased the sensitivity and time resolution of time-resolved crystallography and X-ray scattering measurements. This allows direct visualization of atomic bond formation and breakage, and protein structural changes, during biological reactions.[2] In time-resolved measurements, reactions are often triggered by a short laser pulse, and as a result, photoactivated proteins have become popular targets for these studies.[3−6] The cyanobacteriochrome (CBCR) photoreceptors make up a highly promising family of light-activated proteins for this purpose because of their sensitivity to a range of wavelengths that span the ultraviolet (UV)−visible spectrum and their, comparatively, small size. CBCRs contain a linear bilin chromophore linked to the protein by one or more Cys residues located within a light-sensing domain, known as a GAF domain. It is well documented that the light signaling of CBCRs occurs by photoconversion between two forms of the protein.[7] This photoconversion is initiated by light, which causes an ultrafast (picoseconds) photoisomerization across the C15−C16 bond of the bilin molecule (Figure 1A,B). This, in turn, triggers other localized motions, such as movements of nearby side chains (nanoseconds to microseconds), which finally induce large-scale protein conformational changes (milliseconds to seconds) and, ultimately, the biological signaling response. It has been found that the wavelength sensitivity of CBCRs can be affected by the exact conformation of each of the rings within the bilin (e.g., the so-called trapped-twist geometry), as well as factors such as protonation and hydration,[8] and even the orientation of the D ring of the bilin cofactor, which changes the conjugation of the ring system.[9] On the basis of these recent advances in our understanding of CBCR action, it has now even been suggested that the prediction of photocycles of some CBCRs from sequence alone is possible,[10] and a single CBCR has been rationally redesigned to produce new photoconvertible variants.[11]

The thermophilic cyanobacterium *Thermosynechococcus elongatus* BP-1 contains a number of putative CBCR photoreceptors, one of which, TePixJ, has become a model system for structural studies of this class of protein. TePixJ contains a so-called DXCF motif in which a second Cys residue can link to C10 of the bilin,[12,13] shortening the wavelength of absorbance and thus extending the wavelength range of the phycoviolobilin (PVB) chromophore (Figure 1A,B). As a result, TePixJ converts between blue and green light-absorbing states (known as Pb and Pg states, respectively). The Pb state is the dark-adapted state in which the bilin is in a 15*Z* conformation, with two Cys linkages; the Pg state contains the bilin in a 15*E* conformation with only one Cys linkage. The structures of TePixJ in the Pb and Pg states have been determined using X-ray crystallography[14,15] and solution phase nuclear magnetic resonance.[16] Together, these studies suggest that photoconversion from the Pb to Pg state involves an initial photoisomerization of the bilin cofactor (15*Z* to 15*E*), which is then proposed to trigger a chain of structural changes in the protein. These include the breakage of the C10−Cys-494 thioether bond, opposite rotations of the A and D pyrrole rings, sliding of the bilin in the binding pocket, the appearance of an extended region of disorder that includes Cys-494, and finally changes in the protein backbone (Figure 1C,D).[16] Although direct detection of these processes is still lacking, it has recently been shown that photoactive crystals can now be produced, paving the way for future time-resolved crystallography studies.[17] However, to facilitate such measurements, it is important to understand the entire photoconversion kinetics in detail to ascertain the time scales

Received: May 8, 2020
Revised: July 2, 2020
Published: August 4, 2020

https://dx.doi.org/10.1021/acs.biochem.0c00382
Biochemistry 2020, 59, 2909−2915

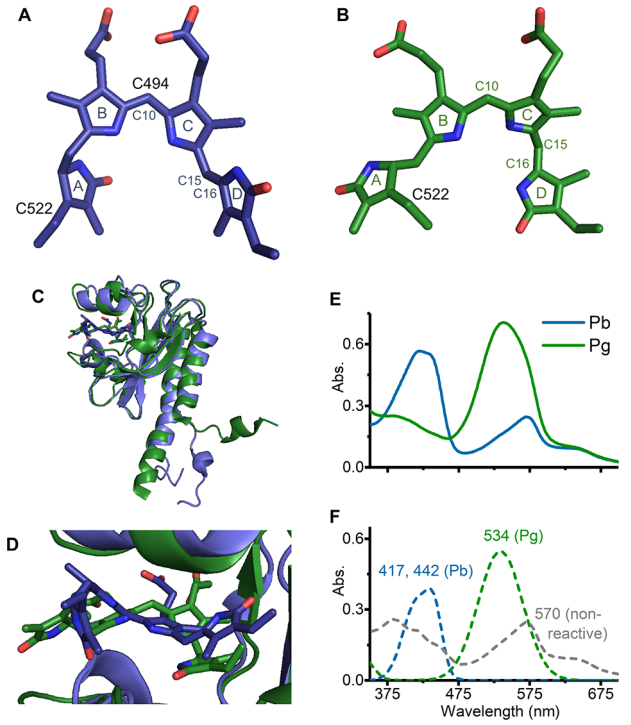

Figure 1. Structures of PVB in (A) Pb and (B) Pg, including labels of significant C atoms, ring labels, and locations of bound Cys residues in the TePixJ CBCR. Atom coloring: blue for N, red for O, and dark blue (Pb) or green (Pg) for C (H atoms are not shown). (C) Superposition of Pb (PDB entry 2M7U) and Pg (PDB entry 2M7V) protein structures. (D) Superposition of the chromophore region of structures shown in panel C. (E) Visible absorbance spectra of the Pb and Pg states. (F) Calculated spectral contributions of Pb, Pg, and nonreactive components derived from spectra shown in panel E (shown in more detail in Figure S1).

of any structural changes in the protein. Here, we have performed, for the first time, time-resolved spectroscopy in the visible and infrared regions on TePixJ to study the kinetics of intermediate formation after photoexcitation. Consequently, we report the photoreactions of both Pb and Pg forms of the protein, which will provide a crucial frame of reference for future time-resolved structural studies.

TePixJ converts between states with major visible absorption features at 417 and 442 nm (Pb) and 534 nm (Pg) (Figure 1E,F and Figure S1), in agreement with previous studies.[12,18] In both states, in addition to the spectral features that change upon illumination, there is some contribution from a nonreactive species that absorbs at 385 and 570 nm (Figure 1F and Figure S1). Previous work on a related CBCR, Tlr1999, has identified a similar nonreactive component as a configuration of PVB that is trapped in the 15*Z* isomer (as in the Pb state) with a nonligated Cys, perhaps due to oxidation of the Cys residue.[19] However, it is also known that TePixJ can contain a mixture of PVB and the phycocyanobilin (PCB) from which it is autocatalytically isomerized,[12] in which case the nonreactive component is likely to be a PCB configuration with limited photoreactivity,[20] and only one Cys linkage.[11] Whatever its identity, this nonreactive species will still absorb light but does not appear to photoconvert between states, and photoexcitation does not give rise to any long-lived states (Figure S2); therefore, it is not likely that it will initiate any changes in protein structure. It has been found that the Pg state of TePixJ shows little to no thermal reversion to the Pb state over several months, so that should not affect any kinetics measured here.[21]

Initially, we studied the kinetics of the forward photoconversion of the Pb (15*Z*) state to the Pg (15*E*) state of TePixJ. After photoexcitation of the Pb state, changes in absorption in the visible region were recorded covering time scales from picoseconds to seconds (Figure 2A−C and Figures S3−S5) and in the infrared region covering time scales from 1 ps to 400 μs (Figure 2D and Figure S6). In the visible region, data up to 3.6 μs were collected on samples in both H_2O and D_2O buffer systems to provide a more direct comparison with the infrared data set (collected in D_2O buffer due to strong infrared absorption of H_2O). Data were analyzed globally with a model of sequentially evolving components to yield evolution-associated difference spectra (EADS) and lifetimes of conversion between the EADS (Figure 2). Data in the visible region display a strong bleach feature of the Pb state (417 and 442 nm) and transient peaks resulting from photoexcited states and subsequent reaction intermediates and products. In the infrared region, a previous resonance Raman study of TePixJ has assigned a feature at ∼1570 cm^{-1} as a N−H in-plane bending mode, strong bands above 1600 cm^{-1} as C═C stretches of ring D, and A−B and C−D methane bridges.[21]

On the basis of these data, it appears that there are a number of distinct steps during the photoconversion of the Pb state to the Pg state. The first transition from EADS1 to EADS2 in the infrared region has a lifetime of 11.9 ps, and in addition to spectral contributions from excited state relaxation processes, a new large positive feature appears at 1654 cm^{-1} and a smaller positive feature appears on the high-frequency side of the major ground state bleach causing an apparent shift in this feature (Figure 2H). This transition is therefore likely to correspond to the 15*Z* to 15*E* photoisomerization. However, it appears that there is a lack of any definite absorption features in the visible region associated with the photoisomerization step. There are no positive features in the visible difference spectra between 1 ns and 1 ms, and the only apparent feature is a bleach of the Pb absorption feature (442 nm). There are two possible explanations for this phenomenon. First, it may be that there is only a small shift in absorbance upon isomerization, and that the new state has an extinction coefficient that is much lower than that of the starting Pb state, as in the case of related DXCF CBCR Tlr1999 where photoisomerization shifts the absorbance maximum by only 2 nm.[19] The second option is that the absorption of the isomerized state may have shifted out of the monitored range, to wavelengths shorter than 400 nm, as in the case of CBCR Tlr0924, where isomerization shifts the Pb peak absorbance from 450 to 390 nm.[22] This second hypothesis is supported by the changes in spectral shape on the short-wavelength side of the bleach during subsequent transitions. Because of the apparent lack of photoisomerized state absorbance in the visible region, the observed EADS1 to EADS2 transition (Figure 2E) is likely to primarily result from relaxation of the photoexcited state, and thus, the transition has very similar lifetimes in H_2O and D_2O (6.4 and 5.9 ps, respectively). The shapes of the EADS for the measurements in the D_2O and H_2O buffer systems are virtually identical (Figure S7), implying that the same chemistry occurs in both cases.

In the visible and infrared data sets, the EADS2 to EADS3 transition (Figure 2E,H), with a lifetime of several hundred

https://dx.doi.org/10.1021/acs.biochem.0c00382
Biochemistry 2020, 59, 2909−2915

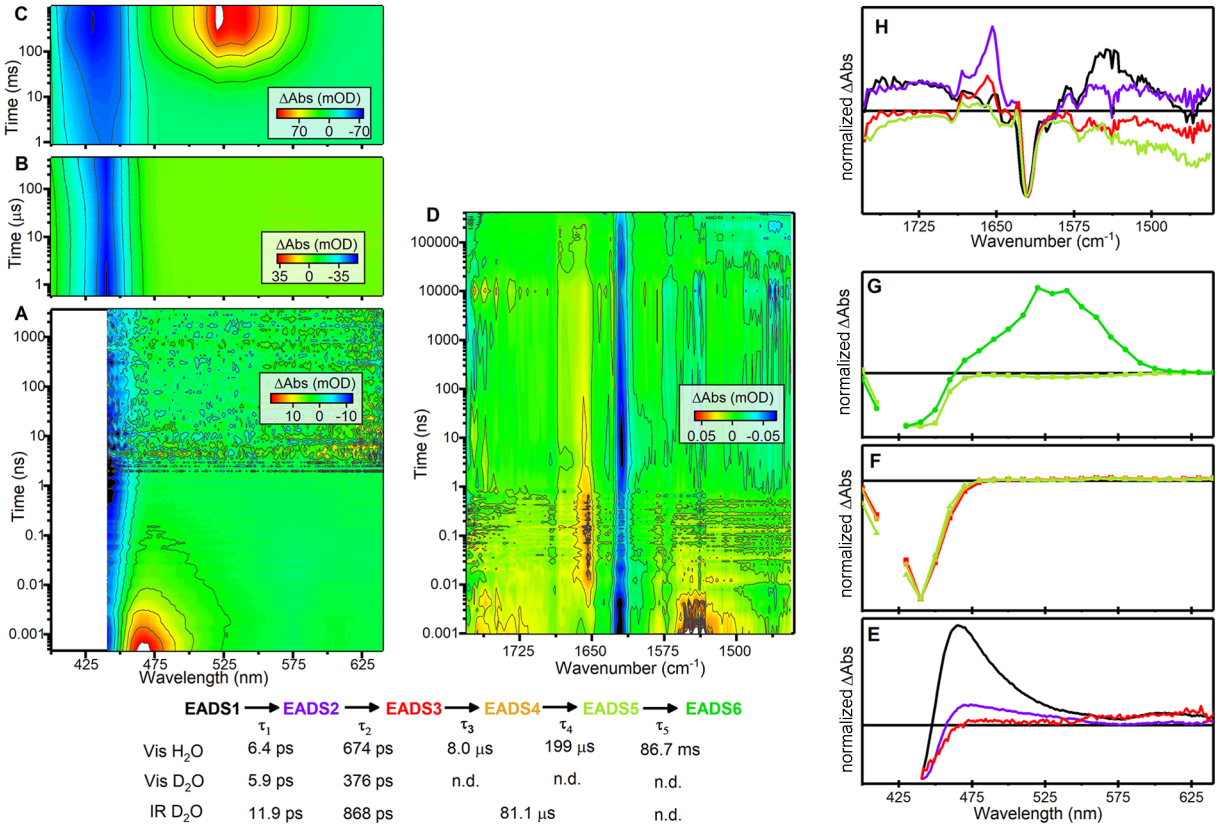

Figure 2. Time-resolved changes after photoexcitation of the Pb state. Visible data sets in H_2O-based buffer (A) from 0.47 ps to 3.9 μs, (B) from 0.6 to 450 μs, and (C) from 0.9 to 994 ms and (D) an infrared data set from 1 ps to 400 μs. Evolution-associated difference spectra (EADS) normalized to the most intense feature, and corresponding lifetimes, from global analysis of (E−G) visible data sets and (H) the infrared data set, shown in more detail in Figures S7−S10. For samples in D_2O, the visible data set extends to 3.9 μs and the infrared data set to 400 μs, so lifetimes for steps beyond these time scales were not determined (n.d.). The blank regions in panels A and E centered at 420 nm are due to an excess of scattered pump light on these time scales, which overwhelms any changes in absorption from the sample.

picoseconds, corresponds to a loss of signal intensity but no distinct spectral changes and is therefore likely to correspond to excited state relaxation. This is followed by a number of subtle spectral changes that occur on the microsecond time scale, suggesting that these steps have a minimal effect on the electronic properties of the bilin cofactor (Figure 2E,F). The visible data can be fitted with two components (8.0 and 199 μs lifetimes), whereas the infrared data could be fitted to only one (81.1 μs), which is likely a convolution of the two steps observed in the visible data that cannot be resolved due to the low signal-to-noise ratio. In the visible region, there are minor changes to the shape of the ground state bleach, and in the infrared region, there is a loss of some of the distinct features that were previously apparent. These may correspond to localized structural changes, perhaps the sliding of the bilin within the active site, that have been observed in previous structural studies.[16] However, as these changes are likely to be spectroscopically silent, it further emphasizes the importance of developing time-resolved structural approaches to obtain a complete molecular description of all steps in the photocycle of these proteins. There is only one further notable spectral transition on slower time scales, the formation of the final Pg state (Figure 2C,G), which occurs with a lifetime of 86.8 ms. This step in the photoconversion, which represents the breakage of the second Cys linkage, also involves any large-scale protein structural changes that are likely to accompany the formation of the final Pg state.

The time scales for the formation and decay of intermediates in the reverse Pg (15*E*) to Pb (15*Z*) photoconversion have also been measured. Changes in absorption after photoexcitation of the Pg state of TePixJ in the visible region were recorded over time scales from picoseconds to milliseconds (Figure 3A−C and Figures S11−S13) and in the infrared region over time scales from 1 ps to 400 μs (Figure 3D and Figure S14). A number of steps can be identified for the Pg to Pb photoconversion based on the EADS resulting from global analysis (Figure 3E−H), and this shows that the conversion between the two states is not simply a reversal of the steps in the Pb to Pg reaction. This situation is similar to the photoreactions of other CBCRs,[22,23] and the related phytochrome photoreceptors,[24] which often have more identifiable steps in one direction than the other. Unlike the 15*Z* to 15*E* isomerization step that resulted in no apparent new visible spectral features, in the 15*E* to 15*Z* isomerization a new feature is formed at ∼561 nm (first apparent in EADS4). This is similar to the absorption of the nonreactive species present in the samples, consistent with those species being 15*Z* isomers trapped in a Pg-like protein environment. The EADS3 to EADS4 transition in which this feature appears in the visible region correlates with changes in the infrared region on similar time scales of several hundred picoseconds. Hence, this is likely to correspond to the isomerization step. There are no new distinct features formed in the infrared region, but it may be that, as with other CBCRs, the isomerization results in a

https://dx.doi.org/10.1021/acs.biochem.0c00382
Biochemistry 2020, 59, 2909−2915

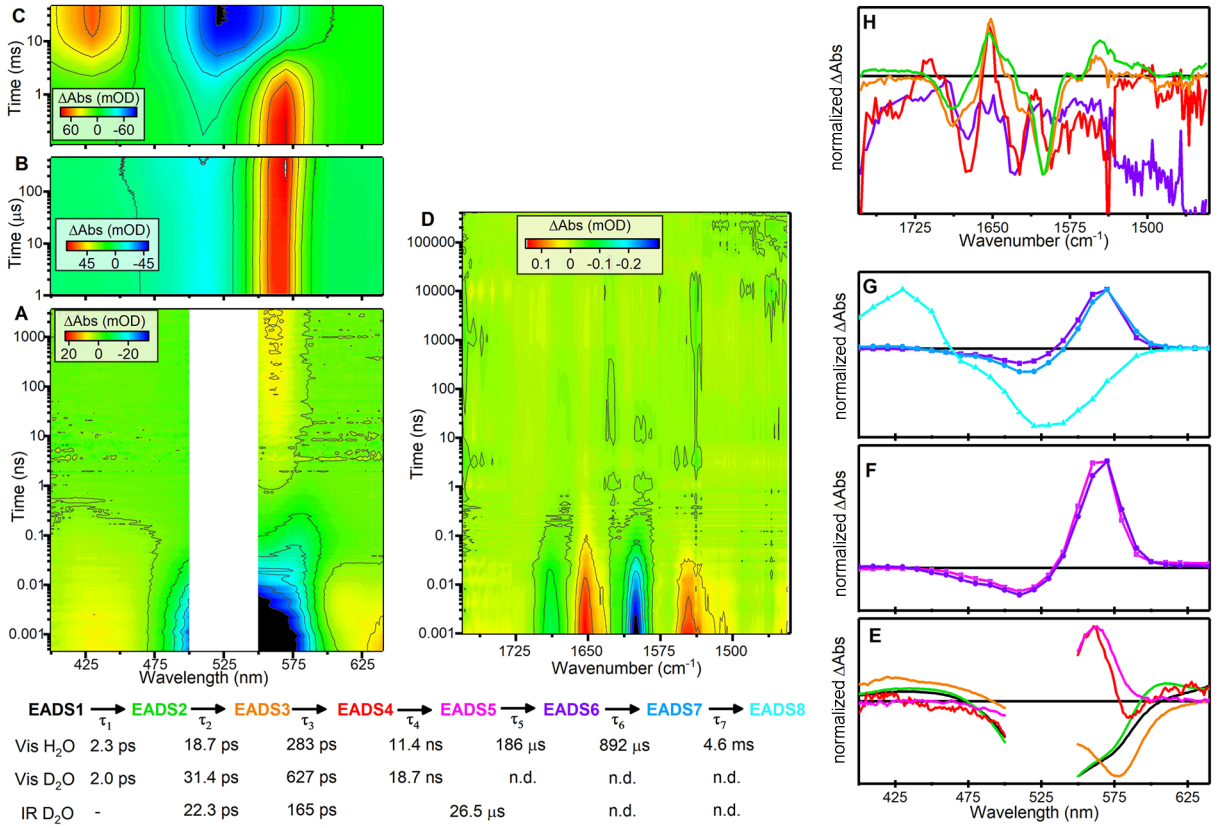

Figure 3. Time-resolved changes after photoexcitation of the Pg state. Visible data sets in H_2O-based buffer (A) from 0.36 ps to 3.6 μs, (B) from 1 to 450 μs, and (C) from 0.1 to 45 ms and (D) infrared data set from 1 ps to 400 μs. Evolution-associated difference spectra (EADS) normalized to the most intense feature, and corresponding lifetimes, from global analysis of (E−G) visible data sets and (H) an infrared data set, shown in more detail in Figures S15−S18. For samples in D_2O, the visible data set extends to 3.6 μs and the infrared data set to 400 μs, so lifetimes for steps beyond these time scales were not determined (n.d.). The blank region in panel A centered at 530 nm is due to an excess of scattered pump light on these time scales, which overwhelms any changes in absorption from the sample.

broadening, rather than clear shift, of features.[25] In addition to the isomerization, there is significant loss of signal intensity for peaks present in EADS1 and EADS2, so the isomerization will occur concurrently with excited state relaxation, as seen in the forward reaction. The *E* to *Z* isomerization occurs more slowly than the *Z* to *E* isomerization, and differences in photoisomerization rates of the forward and reverse reaction have been observed in bilin-containing photoreceptors,[23,26−28] because the interactions of the bilin with the surrounding environment will be different due to structural differences between starting states (e.g., Figure 1) and the activation energy of isomerization will be different in each case. The transitions preceding the isomerization, with lifetimes of around 2 and 20 ps, are therefore likely to derive from excited state relaxation, which correlates with the first observed transition in the infrared (EADS2 to EADS3) that displays no significant change in spectra, only a change in intensity. The excited state lifetimes of other bilin-containing photoreceptors are often reported as multiexponential, which can be explained either as ground state heterogeneity[26] or as the initial excited state affecting the surrounding protein environment.[29]

Over the subsequent nanoseconds and hundreds of microseconds, the infrared data show no signs of significant structural changes occurring, and in the visible region, there are subtle changes in the apparent position and shape of the positive absorption feature of the reaction intermediate; therefore, we assign these changes to subtle changes in the conformation of the bilin within the binding pocket. As with the Pb photoreaction, it appears that the one lifetime resolved from the infrared data (26.5 μs) is a combination of the two steps resolved in the visible data (11.4 ns and 186 μs). The differences between H_2O and D_2O buffer solutions are, as with the Pb photoreaction, purely in the kinetics, not in the chemistry occurring (Figure S15). In the photoconversions of many CBCR and phytochrome proteins, the reactions include deprotonation and the subsequent reprotonation of the bilin chromophore.[24,25,30,31] It has also been hypothesized that deprotonation of the bilin is required to promote the interaction with the neutral thiol group during the formation of the second Cys linkage.[32] The transition from EADS4 to EADS5 displays a moderate kinetic isotope effect (KIE, lifetimes of 18.7 ns in D_2O and 11.4 ns in H_2O), making this a plausible proton transfer step. However, such a step should have a distinct infrared spectral signature,[25] and blue-shifted absorbance maxima,[14,33] neither of which are observed here, so the observed KIE may be due to only changed dynamics due to exchangeable protons making the protein "heavier" and transitions slower.[24] In a manner similar to that of the Pb photoreaction, there are only minor spectral changes on the nanosecond to microsecond time scales, suggesting that they represent localized structural changes with no significant impact on the bilin environment. The formation of the final Pb state, which involves the formation of the second linkage at position C10 of the bilin chromophore to the Cys residue,

https://dx.doi.org/10.1021/acs.biochem.0c00382
Biochemistry 2020, 59, 2909−2915

occurs with a lifetime of 4.9 ms. As with other CBCRs, it appears as though formation of the Cys linkage occurs more rapidly than the breakage of this bond during the reverse step.[23]

In summary, we have used visible and infrared transient absorption measurements to identify the time scales of intermediate formation in the photoconversions of the CBCR TePixJ (Figure 4). It is clear that a number of localized

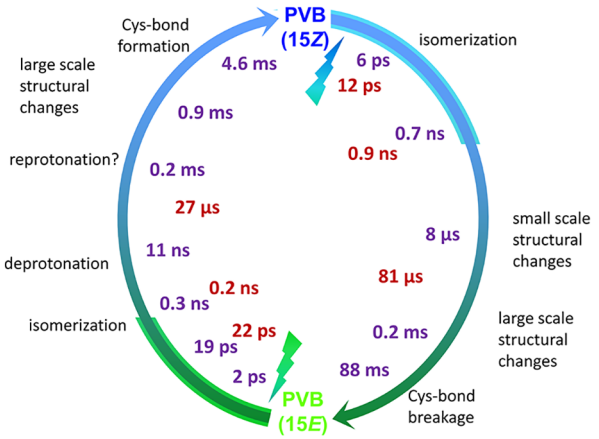

Figure 4. Summary of the lifetimes fitted for the photoconversion of TePixJ. Values from visible transient absorption are colored purple, and those from IR measurements red. Highlighting around the arrows denotes the lifetime of the excited state.

and more large-scale structural changes take place over a wide range of time scales from picoseconds to milliseconds. While it would be expected that large-scale motions would be restricted in a crystalline form, the production of photoconvertible TePixJ crystals[17] implies that any restrictions do not block the overall reaction, and a study of a phytochrome showed overall agreement between crystal and solution phase structural data.[34] Previous X-ray solution scattering studies of phytochrome proteins[24,34,35] found a number of very slow (milliseconds to seconds) large-scale structural changes took place after the final visible spectral transition had occurred; similar large-scale structural changes may take place in TePixJ, although TePixJ contains only a GAF domain, not the PAS-GAF-PHY structure of phytochromes, so large-scale structural changes are likely to be less extensive. Further time-resolved studies to probe millisecond to second changes using vibrational (infrared or Raman) spectroscopy or circular dichroism would provide valuable elucidation of any later reaction steps. The time scales associated with intermediate formation presented here will be crucial to inform any future time-resolved structural studies of this CBCR and other related CBCRs.

■ ASSOCIATED CONTENT

Supporting Information

The Supporting Information is available free of charge at https://pubs.acs.org/doi/10.1021/acs.biochem.0c00382.

Detailed experimental procedures, time-resolved spectroscopy data, and results of global analysis (PDF)

Accession Codes

Cyanobacteriochrome TePixJ, UniProtKB Q8DLC7.

■ AUTHOR INFORMATION

Corresponding Author

Nigel S. Scrutton − *Manchester Institute of Biotechnology and Department of Chemistry, School of Natural Sciences, Faculty of Science and Engineering, The University of Manchester, Manchester M1 7DN, U.K.*; orcid.org/0000-0002-4182-3500; Email: nigel.scrutton@manchester.ac.uk

Authors

Samantha J. O. Hardman − *Manchester Institute of Biotechnology and Department of Chemistry, School of Natural Sciences, Faculty of Science and Engineering, The University of Manchester, Manchester M1 7DN, U.K.*

Derren J. Heyes − *Manchester Institute of Biotechnology and Department of Chemistry, School of Natural Sciences, Faculty of Science and Engineering, The University of Manchester, Manchester M1 7DN, U.K.*

Igor V. Sazanovich − *Central Laser Facility, Research Complex at Harwell, Science and Technology Facilities Council, Didcot OX11 0QX, United Kingdom*

Complete contact information is available at: https://pubs.acs.org/10.1021/acs.biochem.0c00382

Notes

The authors declare no competing financial interest.

■ ACKNOWLEDGMENTS

Time-resolved infrared measurements were performed through program access support of the UK Science and Technology Facilities Council (STFC). Time-resolved visible measurements were performed at the Ultrafast Biophysics Facility, Manchester Institute of Biotechnology, as funded by BBSRC Alert14 Award BB/M011658/1.

■ ABBREVIATIONS

CBCR, cyanobacteriochrome; PVB, phycoviolobilin; Pb, blue light-absorbing; Pg, green light-absorbing; EADS, evolution-associated difference spectra; PDB, Protein Data Bank.

■ REFERENCES

(1) Chergui, M., and Collet, E. (2017) Photoinduced Structural Dynamics of Molecular Systems Mapped by Time-Resolved X-ray Methods. *Chem. Rev. (Washington, DC, U. S.) 117*, 11025−11065.

(2) Levantino, M., Yorke, B. A., Monteiro, D. C. F., Cammarata, M., and Pearson, A. R. (2015) Using synchrotrons and XFELs for time-resolved X-ray crystallography and solution scattering experiments on biomolecules. *Curr. Opin. Struct. Biol. 35*, 41−48.

(3) Tenboer, J., Basu, S., Zatsepin, N., Pande, K., Milathianaki, D., Frank, M., Hunter, M., Boutet, S., Williams, G. J., Koglin, J. E., Oberthuer, D., Heymann, M., Kupitz, C., Conrad, C., Coe, J., Roy-Chowdhury, S., Weierstall, U., James, D., Wang, D., Grant, T., Barty, A., Yefanov, O., Scales, J., Gati, C., Seuring, C., Srajer, V., Henning, R., Schwander, P., Fromme, R., Ourmazd, A., Moffat, K., Van Thor, J. J., Spence, J. C. H., Fromme, P., Chapman, H. N., and Schmidt, M. (2014) Time-resolved serial crystallography captures high-resolution intermediates of photoactive yellow protein. *Science 346*, 1242−1246.

(4) Kupitz, C., Basu, S., Grotjohann, I., Fromme, R., Zatsepin, N. A., Rendek, K. N., Hunter, M. S., Shoeman, R. L., White, T. A., Wang, D., James, D., Yang, J.-H., Cobb, D. E., Reeder, B., Sierra, R. G., Liu, H., Barty, A., Aquila, A. L., Deponte, D., Kirian, R. A., Bari, S., Bergkamp, J. J., Beyerlein, K. R., Bogan, M. J., Caleman, C., Chao, T.-C., Conrad, C. E., Davis, K. M., Fleckenstein, H., Galli, L., Hau-Riege, S. P., Kassemeyer, S., Laksmono, H., Liang, M., Lomb, L., Marchesini, S., Martin, A. V., Messerschmidt, M., Milathianaki, D., Nass, K., Ros, A.,

https://dx.doi.org/10.1021/acs.biochem.0c00382
Biochemistry 2020, 59, 2909−2915

Roy-Chowdhury, S., Schmidt, K., Seibert, M., Steinbrener, J., Stellato, F., Yan, L., Yoon, C., Moore, T. A., Moore, A. L., Pushkar, Y., Williams, G. J., Boutet, S., Doak, R. B., Weierstall, U., Frank, M., Chapman, H. N., Spence, J. C. H., and Fromme, P. (2014) Serial time-resolved crystallography of photosystem II using a femtosecond X-ray laser. *Nature 513*, 261−265.

(5) Heyes, D. J., Hardman, S. J. O., Pedersen, M. N., Woodhouse, J., De La Mora, E., Wulff, M., Weik, M., Cammarata, M., Scrutton, N. S., and Schirò, G. (2019) Light-induced structural changes in a full-length cyanobacterial phytochrome probed by time-resolved X-ray scattering. *Commun. Biol. 2*, 1.

(6) Coquelle, N., Sliwa, M., Woodhouse, J., Schirò, G., Adam, V., Aquila, A., Barends, T. R. M., Boutet, S., Byrdin, M., Carbajo, S., De la Mora, E., Doak, R. B., Feliks, M., Fieschi, F., Foucar, L., Guillon, V., Hilpert, M., Hunter, M. S., Jakobs, S., Koglin, J. E., Kovacsova, G., Lane, T. J., Lévy, B., Liang, M., Nass, K., Ridard, J., Robinson, J. S., Roome, C. M., Ruckebusch, C., Seaberg, M., Thepaut, M., Cammarata, M., Demachy, I., Field, M., Shoeman, R. L., Bourgeois, D., Colletier, J.-P., Schlichting, I., and Weik, M. (2018) Chromophore twisting in the excited state of a photoswitchable fluorescent protein captured by time-resolved serial femtosecond crystallography. *Nat. Chem. 10*, 31−37.

(7) Fushimi, K., and Narikawa, R. (2019) Cyanobacteriochromes: photoreceptors covering the entire UV-to-visible spectrum. *Curr. Opin. Struct. Biol. 57*, 39−46.

(8) Rockwell, N. C., Martin, S. S., Gulevich, A. G., and Lagarias, J. C. (2014) Conserved Phenylalanine Residues Are Required for Blue-Shifting of Cyanobacteriochrome Photoproducts. *Biochemistry 53*, 3118−3130.

(9) Rockwell, N. C., Martin, S. S., and Lagarias, J. C. (2012) Mechanistic Insight into the Photosensory Versatility of DXCF Cyanobacteriochromes. *Biochemistry 51*, 3576−3585.

(10) Rockwell, N. C., Martin, S. S., and Lagarias, J. C. (2015) Identification of DXCF cyanobacteriochrome lineages with predictable photocycles. *Photoch. Photobio. Sci. 14*, 929−941.

(11) Fushimi, K., Hasegawa, M., Ito, T., Rockwell, N. C., Enomoto, G., Win, N.-N., Lagarias, J. C., Ikeuchi, M., and Narikawa, R. (2020) Evolution-inspired design of multicolored photoswitches from a single cyanobacteriochrome scaffold. *Proc. Natl. Acad. Sci. U. S. A. 117*, 15573.

(12) Rockwell, N. C., Martin, S. S., Gulevich, A. G., and Lagarias, J. C. (2012) Phycoviolobilin Formation and Spectral Tuning in the DXCF Cyanobacteriochrome Subfamily. *Biochemistry 51*, 1449−1463.

(13) Rockwell, N. C., Martin, S. S., Feoktistova, K., and Lagarias, J. C. (2011) Diverse two-cysteine photocycles in phytochromes and cyanobacteriochromes. *Proc. Natl. Acad. Sci. U. S. A. 108*, 11854−11859.

(14) Narikawa, R., Ishizuka, T., Muraki, N., Shiba, T., Kurisu, G., and Ikeuchi, M. (2013) Structures of cyanobacteriochromes from phototaxis regulators AnPixJ and TePixJ reveal general and specific photoconversion mechanism. *Proc. Natl. Acad. Sci. U. S. A. 110*, 918−923.

(15) Burgie, E. S., Walker, J. M., Phillips, G. N., Jr., and Vierstra, R. D. (2013) A Photo-Labile Thioether Linkage to Phycoviolobilin Provides the Foundation for the Blue/Green Photocycles in DXCF-Cyanobacteriochromes. *Structure 21*, 88−97.

(16) Cornilescu, C. C., Cornilescu, G., Burgie, E. S., Markley, J. L., Ulijasz, A. T., and Vierstra, R. D. (2014) Dynamic Structural Changes Underpin Photoconversion of a Blue/Green Cyanobacteriochrome Between its Dark and Photoactivated States. *J. Biol. Chem. 289*, 3055−3065.

(17) Burgie, E. S., Clinger, J. A., Miller, M. D., Brewster, A. S., Aller, P., Butryn, A., Fuller, F. D., Gul, S., Young, I. D., Pham, C. C., Kim, I.-S., Bhowmick, A., O'Riordan, L. J., Sutherlin, K. D., Heinemann, J. V., Batyuk, A., Alonso-Mori, R., Hunter, M. S., Koglin, J. E., Yano, J., Yachandra, V. K., Sauter, N. K., Cohen, A. E., Kern, J., Orville, A. M., Phillips, G. N., and Vierstra, R. D. (2020) Photoreversible interconversion of a phytochrome photosensory module in the crystalline state. *Proc. Natl. Acad. Sci. U. S. A. 117*, 300−307.

(18) Ishizuka, T., Shimada, T., Okajima, K., Yoshihara, S., Ochiai, Y., Katayama, M., and Ikeuchi, M. (2006) Characterization of Cyanobacteriochrome TePixJ from a Thermophilic Cyanobacterium Thermosynechococcus elongatus Strain BP-1. *Plant Cell Physiol. 47*, 1251−1261.

(19) Enomoto, G., Hirose, Y., Narikawa, R., and Ikeuchi, M. (2012) Thiol-Based Photocycle of the Blue and Teal Light-Sensing Cyanobacteriochrome Tlr1999. *Biochemistry 51*, 3050−3058.

(20) Ishizuka, T., Kamiya, A., Suzuki, H., Narikawa, R., Noguchi, T., Kohchi, T., Inomata, K., and Ikeuchi, M. (2011) The Cyanobacteriochrome, TePixJ, Isomerizes Its Own Chromophore by Converting Phycocyanobilin to Phycoviolobilin. *Biochemistry 50*, 953−961.

(21) Ulijasz, A. T., Cornilescu, G., von Stetten, D., Cornilescu, C., Velazquez Escobar, F., Zhang, J., Stankey, R. J., Rivera, M., Hildebrandt, P., and Vierstra, R. D. (2009) Cyanochromes Are Blue/Green Light Photoreversible Photoreceptors Defined by a Stable Double Cysteine Linkage to a Phycoviolobilin-type Chromophore. *J. Biol. Chem. 284*, 29757−29772.

(22) Hauck, A. F. E., Hardman, S. J. O., Kutta, R. J., Greetham, G. M., Heyes, D. J., and Scrutton, N. S. (2014) The photoinitiated reaction pathway of full-length cyanobacteriochrome Tlr0924 monitored over twelve orders of magnitude. *J. Biol. Chem. 289*, 17747−17757.

(23) Hardman, S. J. O., Hauck, A. F. E., Clark, I. P., Heyes, D. J., and Scrutton, N. S. (2014) Comprehensive Analysis of the Green-to-Blue Photoconversion of Full-Length Cyanobacteriochrome Tlr0924. *Biophys. J. 107*, 2195−2203.

(24) Choudry, U., Heyes, D. J., Hardman, S. J. O., Sakuma, M., Sazanovich, I. V., Woodhouse, J., De La Mora, E., Pedersen, M. N., Wulff, M., Weik, M., Schiro, G., and Scrutton, N. S. (2018) Photochemical Mechanism of an Atypical Algal Phytochrome. *ChemBioChem 19*, 1036−1043.

(25) Velazquez Escobar, F., Utesch, T., Narikawa, R., Ikeuchi, M., Mroginski, M. A., Gärtner, W., and Hildebrandt, P. (2013) Photoconversion Mechanism of the Second GAF Domain of Cyanobacteriochrome AnPixJ. and the Cofactor Structure of Its Green-Absorbing State. *Biochemistry 52*, 4871−4880.

(26) Kim, P. W., Freer, L. H., Rockwell, N. C., Martin, S. S., Lagarias, J. C., and Larsen, D. S. (2012) Femtosecond Photodynamics of the Red/Green Cyanobacteriochrome NpR6012g4 from Nostoc punctiforme. 1. Forward Dynamics. *Biochemistry 51*, 608−618.

(27) Kim, P. W., Freer, L. H., Rockwell, N. C., Martin, S. S., Lagarias, J. C., and Larsen, D. S. (2012) Femtosecond Photodynamics of the Red/Green Cyanobacteriochrome NpR6012g4 from Nostoc punctiforme. 2. Reverse Dynamics. *Biochemistry 51*, 619−630.

(28) Bischoff, M., Hermann, G., Rentsch, S., and Strehlow, D. (2001) First steps in the phytochrome phototransformation: A comparative femtosecond study on the forward (Pr -> Pfr) and back reaction (Pfr -> Pr). *Biochemistry 40*, 181−186.

(29) Slavov, C., Fischer, T., Barnoy, A., Shin, H., Rao, A. G., Wiebeler, C., Zeng, X., Sun, Y., Xu, Q., Gutt, A., Zhao, K.-H., Gärtner, W., Yang, X., Schapiro, I., and Wachtveitl, J. (2020) The interplay between chromophore and protein determines the extended excited state dynamics in a single-domain phytochrome. *Proc. Natl. Acad. Sci. U. S. A. 117*, 16356.

(30) Velazquez Escobar, F., Piwowarski, P., Salewski, J., Michael, N., Fernandez Lopez, M., Rupp, A., Qureshi, B. M., Scheerer, P., Bartl, F., Frankenberg-Dinkel, N., Siebert, F., Andrea Mroginski, M., and Hildebrandt, P. (2015) A protonation-coupled feedback mechanism controls the signalling process in bathy phytochromes. *Nat. Chem. 7*, 423−430.

(31) Borucki, B., von Stetten, D., Seibeck, S., Lamparter, T., Michael, N., Mroginski, M. A., Otto, H., Murgida, D. H., Heyn, M. P., and Hildebrandt, P. (2005) Light-induced Proton Release of Phytochrome Is Coupled to the Transient Deprotonation of the Tetrapyrrole Chromophore. *J. Biol. Chem. 280*, 34358−34364.

(32) Sato, T., Kikukawa, T., Miyoshi, R., Kajimoto, K., Yonekawa, C., Fujisawa, T., Unno, M., Eki, T., and Hirose, Y. (2019)

https://dx.doi.org/10.1021/acs.biochem.0c00382
Biochemistry 2020, 59, 2909−2915

Protochromic absorption changes in the two-cysteine photocycle of a blue/orange cyanobacteriochrome. *J. Biol. Chem. 294*, 18909.
(33) Foerstendorf, H., Parbel, A., Scheer, H., and Siebert, F. (1997) Z,E isomerization of the alpha-84 phycoviolobilin chromophore of phycoerythrocyanin from Mastigocladus laminosus investigated by Fourier-transform infrared difference spectroscopy. *FEBS Lett. 402*, 173−176.
(34) Takala, H., Björling, A., Berntsson, O., Lehtivuori, H., Niebling, S., Hoernke, M., Kosheleva, I., Henning, R., Menzel, A., Ihalainen, J. A., and Westenhoff, S. (2014) Signal amplification and transduction in phytochrome photosensors. *Nature 509*, 245−248.
(35) Björling, A., Berntsson, O., Lehtivuori, H., Takala, H., Hughes, A. J., Panman, M., Hoernke, M., Niebling, S., Henry, L., Henning, R., Kosheleva, I., Chukharev, V., Tkachenko, N. V., Menzel, A., Newby, G., Khakhulin, D., Wulff, M., Ihalainen, J. A., and Westenhoff, S. (2016) Structural photoactivation of a full-length bacterial phytochrome. *Science Advances 2*, No. e1600920.

https://dx.doi.org/10.1021/acs.biochem.0c00382
Biochemistry 2020, 59, 2909−2915